2016 IEEE Conference on Control Applications (CCA)
Part of 2016 IEEE Multi-Conference on Systems and Control
September 19-22, 2016. Buenos Aires, Argentina

Discrete LQG/LTR Control Augmented by Integrators Applied to a 2-DOF Helicopter

Fernando S. Barbosa[1], Gabriel P. das Neves[2] and Bruno A. Angélico[3]

Abstract— **Linear Quadratic Gaussian (LQR) controller and Kalman Filter (KF) both are robust when acting separately, but this property is lost if using them together. Therefore, a Loop Transfer Recovery (LTR) is made aiming to recover this robustness. This same statement is valid for discrete time LQG/LTR, and this work presents its application in a 2-DOF helicopter. The complete mathematical modeling is developed using Lagrange's method and the system is linearized around the operating point. Digital LQG/LTR control project is made along with integrator insertion to the plant inputs. This helicopter is an interesting plant, allowing the study of many subjects, such as Kalman Filters, sensor fusion, modeling techniques and classical control. Simulation and practical results are presented, showing the controller effectiveness.**

I. INTRODUCTION

A 2 degrees-of-freedom helicopter is a highly non-linear coupled MIMO (Multiple Input, Multiple Output) system [1]. The plant is controlled by two rotors, each composed by a brushless DC motor and a propeller, allowing the helicopter to rotate around two axes, pitch and yaw. The study of such system is a great start to the world of aerial vehicles.

A past work presents the complete system modeling and controls based on DK-iteration [2] using a helicopter made by Quanser. The work presented in [3] shows the construction of a similar helicopter from scratch and goes through the modeling and tests. [4] develops a more accurate model also using Euler-Lagrange equations and designs two control loops, one for each axis, based on observers. [5] develops a 6-DOF IMU (Inertial Measurement Unit) using Kalman Sensor Fusion. More recently, [6] makes use of model free controller with type-2 fuzzy neural networks and elliptic type-2 fuzzy membership functions and proves this kind of controller is able to track both inputs with zero steady state error.

Despite linear quadratic regulator (LQR) and Kalman filter (KF) being robust structures, there is no guarantee of robustness for their simultaneous use [7], which constitutes the linear quadratic Gaussian (LQG) controller. Loop transfer recovery (LTR) is a technique used to make LQG robust again, resulting in the LQG/LTR controller [8][9].

The technical literature about the discrete version of the LQG/LTR controller is not extensive. It is used in [10] to control a disk drive servo system. The asymptotic recovery in minimum phase system is showed in [11]. As integrator insertion is in common use, [12] showed that full convergence cannot be achieved when the integrator is discretized by using the forward Euler method, but it is still possible if the backward Euler approximation is considered instead.

This article starts presenting the system modeling using Euler-Lagrange, resulting in both linear and non-linear equations. Then, discrete LQG/LTR theory is presented along with the controller for the helicopter, followed by its simulation, results and conclusion.

The authors would like to thank Programa de Excelência Acadêmica (Proex) from Coordenação de Aperfeiçoamento de Pessoal de Nvel Superior (CAPES) for the grant 0212083. Yet, we also thank Kennedy X. B. Peixoto for his incredible work and help building the helicopter and Freescale for donating FRDM-K64F development platforms.

The authors are with Dept. Engenharia Telecomunicações e Controle, Escola Politécnica da Universidade de São Paulo, Brasil
[1]barbosa.fs@usp.br
[2]gabriel.pereira.neves@usp.br
[3]angelico@lac.usp.br

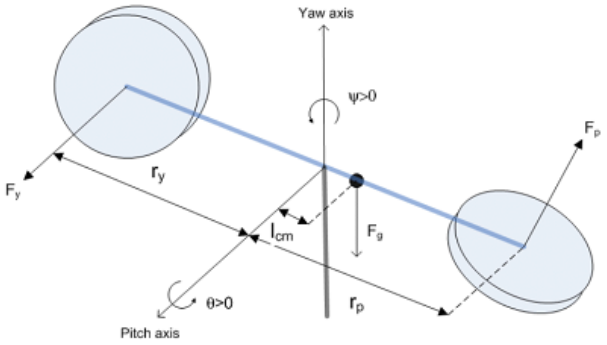

Fig. 1. Simple free-body diagram. Adapted from [1]

II. MODELING

The modeling process presented here follows the same as shown in [2] using the Lagrangian method. The system can rotate around two axes, pitch and yaw (θ and ψ) as Figure 1 presents, with the following convention:

1) Helicopter is horizontal with $\theta = 0$;
2) $\dot{\theta}$ is positive when the nose is moving upwards;
3) $\dot{\psi}$ is positive when the helicopter rotates clockwise;
4) There is neither rolling nor axial movements.

This helicopter is controlled by two brushless DC motors with 9-inch propellers, each generating torque to both axes. For example, the pitch motor controls directly the pitch angle using the force generated by its propeller, creating a torque in yaw as effect of air resistance, characterizing a coupled plant. That said, pitch and yaw resulting torques are written as

$$\tau_p = K_{pp}V_{m\_p} + K_{py}V_{m\_y} \quad (1)$$

$$\tau_y = K_{yy}V_{m\_y} + K_{yp}V_{m\_p} \quad (2)$$

where K_{pp} is the pitch motor torque constant in pitch axis, K_{py} is the yaw motor torque constant in pitch axis, K_{yp} is the pitch motor torque constant in yaw axis, K_{yy} is the yaw

motor torque constant in yaw axis, V_{m_p} is the pitch motor percentage, V_{m_y} is the yaw motor percentage, in which this percentage is related to the signal sent to the motor controller.

Since Lagrangian procedure uses the system energy to derive movement equations, it is a good modeling start. This plant's only potential energy is due to pitch angle, then

$$E_P = m_{heli} g l_{cm} \sin\theta, \tag{3}$$

with m_{heli} being the helicopter total moving mass, g gravity and l_{cm} the center of mass distance to origin. The total kinetic energy is

$$\begin{aligned} E_K = & \frac{1}{2} J_{eq\_p} \dot{\theta}^2 + \frac{1}{2} J_{eq\_y} \dot{\psi}^2 + \\ & \frac{1}{2} m_{heli} \Big[\big(-\sin(\psi)\dot{\psi}\cos(\theta) l_{cm} - \cos(\psi)\sin(\theta)\dot{\theta} l_{cm}\big)^2 \\ & + \big(-\cos(\psi)\dot{\psi}\cos(\theta) l_{cm} + \sin(\psi)\sin(\theta)\dot{\theta} l_{cm}\big)^2 \\ & + \cos(\theta)^2 \dot{\theta}^2 l_{cm}^2 \Big]. \end{aligned} \tag{4}$$

J_{eq_p} and J_{eq_y} are the equivalent moment of inertia related to pitch and yaw, respectively. The generalized forces vector is given by

$$\begin{aligned} Q = & \big[K_{pp} V_{m\_p} + K_{py} V_{m\_y} - B_p \dot{\theta}, \\ & K_{yy} V_{m\_y} + K_{yp} V_{m\_p} - B_y \dot{\psi}\big] \end{aligned} \tag{5}$$

with B_p and B_y as the movement resistance acting above pitch and yaw axes, respectively. Lagrange's equation is

$$\begin{aligned} \frac{\partial}{\partial t}\frac{\partial L}{\partial \dot{\theta}} - \frac{\partial}{\partial \theta} L &= Q_1 \\ \frac{\partial}{\partial t}\frac{\partial L}{\partial \dot{\psi}} - \frac{\partial}{\partial \psi} L &= Q_2 \end{aligned} \tag{6}$$

where L is the Lagrangian of the system, defined by the difference between the total kinetic energy and the total potential energy of the system.

Solving the Euler-Lagrange's equation results in a non-linear equation of motion:

$$\ddot{\theta} = \frac{K_{pp} V_{m\_p} + K_{py} V_{m\_y} - \big(B_p \dot{\theta} + \alpha + \beta\big)}{J_{eq\_p} + m_{heli} l_{cm}^2} \tag{7}$$

$$\alpha = m_{heli} l_{cm}^2 \dot{\psi}^2 \sin(\theta)\cos(\theta) \tag{8}$$

$$\beta = m_{heli} g \cos(\theta) l_{cm} \tag{9}$$

$$\ddot{\psi} = \frac{K_{yp} V_{m\_p} + K_{yy} V_{m\_y} + \gamma - B_y \dot{\psi}}{J_{eq\_y} + m_{heli}\cos(\theta)^2 l_{cm}^2} \tag{10}$$

$$\gamma = 2 m_{heli} l_{cm}^2 \sin(\theta)\cos(\theta)\dot{\psi}\dot{\theta}. \tag{11}$$

Linearizing the system for small angles, as $\theta = 0$ is the operating point, the equations of motion are defined by

$$\ddot{\theta} = \frac{K_{pp} V_{m\_p} + K_{py} V_{m\_y} - B_p \dot{\theta} - m_{heli} g l_{cm}}{J_{eq\_p} + m_{heli} l_{cm}^2} \tag{12}$$

$$\ddot{\psi} = \frac{K_{yp} V_{m\_p} + K_{yy} V_{m\_y} - B_y \dot{\psi}}{J_{eq\_y} + m_{heli} l_{cm}^2}. \tag{13}$$

A state-space system is written based on these equations, resulting in:

$$\dot{x}(t) = Ax(t) + Bu(t) \tag{14}$$

$$y(t) = Cx(t) \tag{15}$$

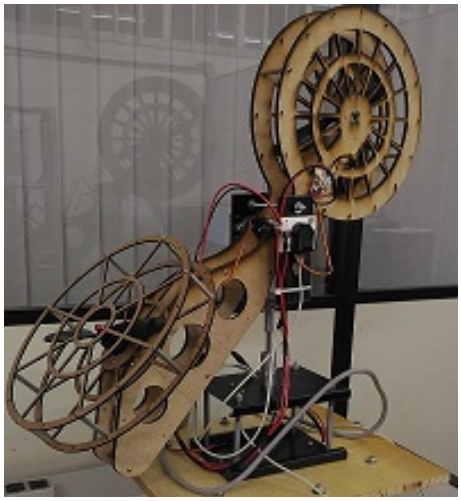

Fig. 2. 2DOF Helicopter built.

where $x(t)$ corresponds to system states and $u(t)$ the motors percentage inputs, defined by

$$x = \begin{bmatrix} \theta & \psi & \dot{\theta} & \dot{\psi} \end{bmatrix}^T \quad \text{and} \quad u = \begin{bmatrix} V_{m\_p} & V_{m\_p} \end{bmatrix}^T. \tag{16}$$

The matrices A, B and C, then, are written as

$$A = \begin{bmatrix} 0 & 0 & 1 & 0 \\ 0 & 0 & 0 & 1 \\ 0 & 0 & \frac{-B_p}{J_{eq\_p} + m_{heli} l_{cm}^2} & 0 \\ 0 & 0 & 0 & \frac{-B_y}{J_{eq\_y} + m_{heli} l_{cm}^2} \end{bmatrix}$$

$$B = \begin{bmatrix} 0 & 0 \\ 0 & 0 \\ \frac{K_{pp}}{J_{eq\_p} + m_{heli} l_{cm}^2} & \frac{K_{py}}{J_{eq\_p} + m_{heli} l_{cm}^2} \\ \frac{K_{yp}}{J_{eq\_y} + m_{heli} l_{cm}^2} & \frac{K_{yy}}{J_{eq\_y} + m_{heli} l_{cm}^2} \end{bmatrix}$$

$$C = \begin{bmatrix} 1 & 0 & 0 & 0 \\ 0 & 1 & 0 & 0 \end{bmatrix}.$$

A. Helicopter Parameters

A 2-DOF helicopter was built in order to test different kinds of controllers as well as decoupling techniques and IMU sensor fusion. Its final version is shown in Figure 2.

Either for the controller development or for simulation, the parameters of the plant have to be measured. To measure the rotors parameters, i.e., the relation between input percentage and thrust/torque generated, the system presented in Figure 3 was also built. It can be used in two configurations:

- Thrust mode: the force (F) generated by the propeller in the axial direction is directly measured on the digital scale. As the modeling process uses the torque relative to the axis, it is enough to multiply this force by the distance of the motor to the coordinate system origin at the helicopter.
- Torque mode: the rotor is placed on the side of the structure such that the thrust does not influence the measurements. The value read on the scale (F) is proportional to the motor reaction torque (M).

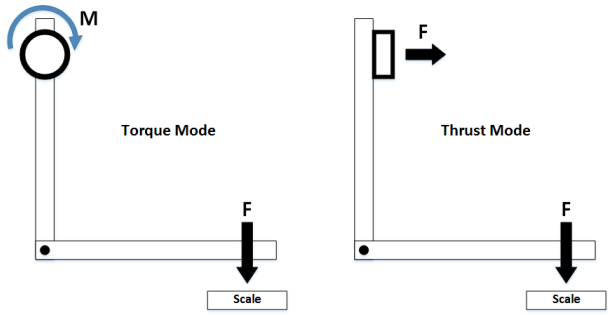

Fig. 3. Motor-propeller test rig.

Table I contains the system parameters, in which some were obtained by linearizing thrust and torque equations and others by simple system identification.

TABLE I
HELICOPTER PARAMETERS

Parameter	Value	Unit
m_{heli}	1.317	kg
l_{cm}	0.038	m
K_{pp}	0.0180	$N.m/\%$
K_{yy}	-0.0033	$N.m/\%$
K_{py}	$-6.35 \cdot 10^{-4}$	$N.m/\%$
K_{yp}	$10.76 \cdot 10^{-4}$	$N.m/\%$
B_p	0.1	$N/\%$
B_y	0.1	$N/\%$
J_{eq_p}	0.384	$kg.m^2$
J_{eq_q}	0.0432	$kg.m^2$

III. DISCRETE LQG/LTR

Consider a discrete, time invariant, linear dynamic system described by

$$\begin{aligned} \mathbf{x}[n+1] &= \Phi\mathbf{x}[n]+\Gamma\mathbf{u}[n]+\Psi\mathbf{w}[n] \\ \mathbf{y}[n] &= \mathbf{C}\mathbf{x}[n]+\mathbf{v}[n], \end{aligned} \tag{17}$$

with $\mathbf{w}[n]$ and $\mathbf{v}[n]$ representing, respectively, the process and measurement noises, both been characterized as additive white Gaussian noise.

It is also assumed that (Φ, Γ) is controllable, (Φ, $\mathbf{C}$) is observable and the system has a square transfer function matrix and no non-minimum phase zero. The transfer function of the nominal system is given by:

$$\mathbf{G}_N(z) = \mathbf{C}(z\mathbf{I}-\Phi)^{-1}\Gamma. \tag{18}$$

Since the controller part is defined by the linear quadratic regulator (LQR), its cost function may be written as

$$J_{\text{LQR}} = \frac{1}{2}\sum_{n=0}^{\infty}\left(\mathbf{x}^\top[n]\mathbf{Q}_\mathbf{x}\mathbf{x}[n]+\mathbf{u}^\top[n]\mathbf{R}_\mathbf{u}\mathbf{u}[n]\right), \tag{19}$$

being $\mathbf{R}_\mathbf{u}$ and $\mathbf{Q}_\mathbf{x}$ the weighting matrices regarding the control efforts and the states, respectively. The optimal control matrix $\mathbf{K}$ is given by

$$\mathbf{K} = (\mathbf{R}_\mathbf{u}+\Gamma^\top\mathbf{P}\Gamma)^{-1}\Gamma^\top\mathbf{P}\Phi, \tag{20}$$

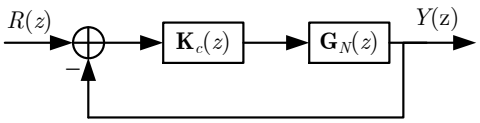

Fig. 4. Kc.

with $\mathbf{P}$ being the solution of the following

$$\Phi^\top(\mathbf{P}-\mathbf{P}\Gamma(\mathbf{R}_\mathbf{u}+\Gamma^\top\mathbf{P}\Gamma)^{-1}\Gamma^\top\mathbf{P})\Phi+\mathbf{Q}_\mathbf{x}=\mathbf{P}. \tag{21}$$

As LQR cheap control structure was chosen, $\mathbf{R}_\mathbf{u}=\rho\mathbf{I}$ and $\mathbf{Q}_\mathbf{x}=\mathbf{C}^\top\mathbf{C}$. Therefore, it is possible to prove that $\mathbf{P}=\mathbf{C}^\top\mathbf{C}$ solves (21) by assuming $\rho=0$ and $\det(\mathbf{C}^\top\mathbf{C})\neq 0$:

$$\begin{aligned} \mathbf{C}^\top\mathbf{C} &= \Phi^\top(\mathbf{P}-\mathbf{P}\Gamma(\mathbf{R}_\mathbf{u}+\Gamma^\top\mathbf{P}\Gamma)^{-1}\Gamma^\top\mathbf{P})\Phi+\mathbf{Q}_\mathbf{x} \\ &= \Phi^\top(\mathbf{C}^\top\mathbf{C}-\mathbf{C}^\top\mathbf{C})\Phi+\mathbf{C}^\top\mathbf{C}=\mathbf{C}^\top\mathbf{C}. \end{aligned} \tag{22}$$

Thus, $\mathbf{K}$ is rewritten as

$$\begin{aligned} \mathbf{K} &= (\Gamma^\top\mathbf{P}\Gamma)^{-1}\Gamma^\top\mathbf{P}\Phi \\ &= (\Gamma^\top\mathbf{C}^\top\mathbf{C}\Gamma)^{-1}\Gamma^\top\mathbf{C}^\top\mathbf{C}\Phi=(\mathbf{C}\Gamma)^{-1}\mathbf{C}\Phi. \end{aligned} \tag{23}$$

Moving to the observer part, Kalman Filter transfer function is given by

$$\mathbf{G}_{KF} = \mathbf{C}(z\mathbf{I}-\Phi)^{-1}\Phi\mathbf{L}_c, \tag{24}$$

where $\mathbf{L}_c$ is the gain matrix of the Kalman filter, calculated as

$$\mathbf{L}_c = \mathbf{Y}\mathbf{C}^\top(\mu\mathbf{I}+\mathbf{C}\mathbf{Y}\mathbf{C}^\top)^{-1}, \tag{25}$$

in which $\mathbf{Y}$ is the solution of the discrete time arithmetic Riccati equation (ARE) [13]

$$\Phi(\mathbf{Y}-\mathbf{Y}\mathbf{C}^\top(\mu\mathbf{I}+\mathbf{C}\mathbf{Y}\mathbf{C}^\top)^{-1}\mathbf{C}\mathbf{Y})\Phi^\top+\Psi\Psi^\top=\mathbf{Y} \tag{26}$$

by choosing $\mathbf{R}_\mathbf{v}=\mu\mathbf{I}$ and $\mathbf{R}_\mathbf{w}=\mathbf{I}$.

Consider a controller with the structure presented in Figure 4 and $\mathbf{G}_N(z)$ the nominal system model, as (18). From the current value estimator, it is defined

$$\hat{\mathbf{x}}[n] = \bar{\mathbf{x}}[n]+\mathbf{L}_c\left(\mathbf{y}[n]-\mathbf{C}\bar{\mathbf{x}}[n]\right) \tag{27}$$

and

$$\bar{\mathbf{x}}[n] = \Phi\hat{\mathbf{x}}[n-1]+\Gamma\mathbf{u}[n-1]. \tag{28}$$

As the LQR controller has the form $\mathbf{u}[n]=-\mathbf{K}\hat{\mathbf{x}}[n]$, it follows that

$$\begin{aligned} \hat{\mathbf{u}}[n+1] &= -\mathbf{K}\left[\bar{\mathbf{x}}[n+1]+\mathbf{L}_c\left(\mathbf{y}[n+1]-\mathbf{C}\bar{\mathbf{x}}[n+1]\right)\right] \\ &= -\mathbf{K}\left(\mathbf{I}-\mathbf{L}_c\mathbf{C}\right)\left(\Phi\hat{\mathbf{x}}[n]-\Gamma\mathbf{K}\hat{\mathbf{x}}[n]\right)-\mathbf{K}\mathbf{L}_c\mathbf{y}[n+1]. \end{aligned} \tag{29}$$

So, it is not hard to show that

$$\hat{\mathbf{x}}[n+1] = \left(\mathbf{I}-\mathbf{L}_c\mathbf{C}\right)\left(\Phi-\Gamma\mathbf{K}\right)\hat{\mathbf{x}}[n]+\mathbf{L}_c\mathbf{y}[n+1]. \tag{30}$$

Applying z-transform to (30), assuming $\mathbf{R}(z)=0$, i.e., $\mathbf{E}(z)=-\mathbf{Y}(z)$, and since $\mathbf{U}(z)=-\mathbf{K}\hat{\mathbf{X}}(z)$:

$$\mathbf{U}(z) = z\mathbf{K}[z\mathbf{I}-(\mathbf{I}-\mathbf{L}_c\mathbf{C})(\Phi-\Gamma\mathbf{K})]^{-1}\mathbf{L}_c\mathbf{E}(z). \tag{31}$$

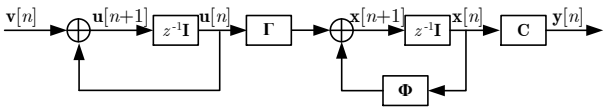

Fig. 5. Augmented plant with integrator using forward Euler discretization.

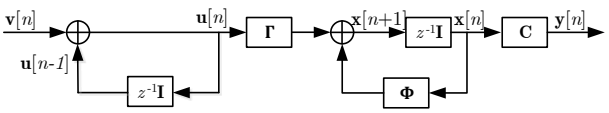

Fig. 6. Augmented plant with backward Euler integrator.

Finally, $\mathbf{K}_c$ is written as

$$\mathbf{K}_c = z\mathbf{K}(z\mathbf{I} - (\mathbf{I} - \mathbf{L}_c\mathbf{C})(\Phi - \Gamma\mathbf{K}))^{-1}\mathbf{L}_c. \quad (32)$$

Theorem 1 (Loop Transfer Recovery [14]): By defining

$$\Delta(z) = \mathbf{G}_N(z)\mathbf{K}_c(z) - \mathbf{G}_{KF}(z), \quad (33)$$

if $\mathbf{G}_N(z)$ is a minimum phase system and $\det(\mathbf{C}\Gamma) \neq 0$, then

$$\rho = 0 \rightarrow \Delta(z) = 0, \quad (34)$$

i.e., the open loop converges to the target loop when ρ approaches zero.

Proof: If $\rho = 0$ and $\det(\mathbf{C}\Gamma) \neq 0$, equation (23) proves that $\mathbf{K} = (\mathbf{C}\Gamma)^{-1}\mathbf{C}\Phi$. By using this result, one can write

$$\mathbf{G}_N(z)\mathbf{K}_c(z) = \mathbf{C}(z\mathbf{I} - \Phi)^{-1}z\Pi\Phi(z\mathbf{I} - (\mathbf{I} - \Pi)\Phi)^{-1}\mathbf{L}_c, \quad (35)$$

where $\Pi = \Gamma(\mathbf{C}\Gamma)^{-1}\mathbf{C}$. Replacing (35) and (24) in (33) gives

$$\Delta(z) = -\mathbf{C}(\mathbf{I} - \Pi)(z\mathbf{I} - \Phi(\mathbf{I} - \Pi))^{-1}\Phi\mathbf{L}_c = 0, \quad (36)$$

since

$$\mathbf{C}(\mathbf{I} - \Pi) = \mathbf{C}(\mathbf{I} - \Gamma(\mathbf{C}\Gamma)^{-1}\mathbf{C}) = 0. \quad (37)$$

■

It is fairly common inserting integrators to the plants input for dealing with steady-state error. The discrete time integrator is generally obtained using the forward or the backward Euler approach. Considering the forward approach, the equivalent system is represented in Figure 5.

The augmented system is:

$$\begin{bmatrix}\mathbf{u}[n+1]\\ \mathbf{x}[n+1]\end{bmatrix} = \underbrace{\begin{bmatrix}\mathbf{I} & \mathbf{0}\\ \Gamma & \Phi\end{bmatrix}}_{\Phi_A}\begin{bmatrix}\mathbf{u}[n]\\ \mathbf{x}[n]\end{bmatrix} + \underbrace{\begin{bmatrix}\mathbf{I}\\ \mathbf{0}\end{bmatrix}}_{\Gamma_A}\mathbf{v}[n] \quad (38)$$

$$\mathbf{y}[n] = \underbrace{\begin{bmatrix}\mathbf{0} & \mathbf{C}\end{bmatrix}}_{\mathbf{C_A}}\begin{bmatrix}\mathbf{u}[n]\\ \mathbf{x}[n]\end{bmatrix}. \quad (39)$$

Defining the augmented matrices as Φ_A, Γ_A and $\mathbf{C_A}$, it does not satisfy Theorem 1, since

$$\det(\mathbf{C_A}\Gamma_A) = \det\left(\begin{bmatrix}\mathbf{0} & \mathbf{C}\end{bmatrix}\begin{bmatrix}\mathbf{I}\\ \mathbf{0}\end{bmatrix}\right) = 0. \quad (40)$$

Considering now the backward Euler, Figure 6, the augmented system is:

$$\begin{bmatrix}\mathbf{u}[n+1]\\ \mathbf{x}[n+1]\end{bmatrix} = \underbrace{\begin{bmatrix}\mathbf{I} & \mathbf{0}\\ \Gamma & \Phi\end{bmatrix}}_{\Phi_B}\begin{bmatrix}\mathbf{u}[n]\\ \mathbf{x}[n]\end{bmatrix} + \underbrace{\begin{bmatrix}\mathbf{I}\\ \Gamma\end{bmatrix}}_{\Gamma_B}\mathbf{v}[n]. \quad (41)$$

Now, *Theorem 1* is satisfied, because $\mathbf{C_B} = \mathbf{C_A}$ and

$$\det(\mathbf{C_B}\Gamma_B) = \det\left(\begin{bmatrix}\mathbf{0} & \mathbf{C}\end{bmatrix}\begin{bmatrix}\mathbf{I}\\ \Gamma\end{bmatrix}\right) \neq 0 \iff \mathbf{C} \neq 0, \Gamma \neq 0.$$

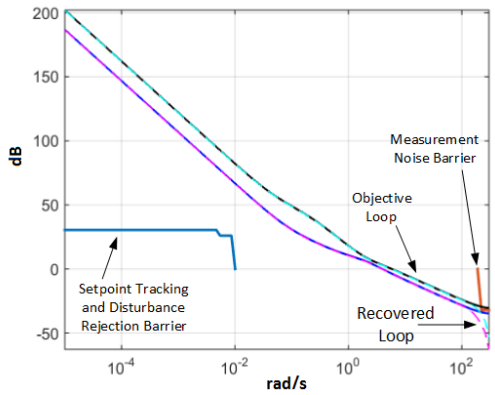

Fig. 7. System barriers together with objetive and recovered loops.

A. Helicopter application

The linear system presented in Section II was discretized using zero-order hold and 100Hz sampling frequency, resulting in the following matrices:

$$\Phi = \begin{bmatrix}1 & 0 & 0.0100 & 0\\ 0 & 1 & 0 & 0.0099\\ 0 & 0 & 0.9974 & 0\\ 0 & 0 & 0 & 0.9781\end{bmatrix}, \quad (42)$$

$$\Gamma = \begin{bmatrix}2.33\cdot10^{-6} & -8.22\cdot10^{-8}\\ 1.18\cdot10^{-6} & -3.65\cdot10^{-6}\\ 4.66\cdot10^{-4} & -1.64\cdot10^{-5}\\ 2.36\cdot10^{-4} & -7.27\cdot10^{-4}\end{bmatrix}. \quad (43)$$

Then, assuming all parameters have $\pm 10\%$ error, low and high frequency barriers were generated. The low-frequency one stands for setpoint tracking and disturbance rejection, and the high-frequency for measurement noise rejection. They are shown in Figure 7.

Since it is desired to guarantee null steady-state error, backward Euler integrator was used. For controller design it is necessary to choose values for ρ, μ and $\mathbf{L}_c$.

The first one to be adjusted is $\mathbf{L}_c$, as it composes the target loop together with μ. It is shown in [12] a suggestion of this matrix. However, $(\Phi - \mathbf{I})$ is not invertible, preventing the use of this hint. Therefore, $\mathbf{L}_c$ was manually set as

$$\mathbf{L}_c = \begin{bmatrix}1 & -0.1 & 0.1 & -0.1 & 1 & 1\\ -0.1 & 1 & -0.1 & 1 & 0 & -3\end{bmatrix}^T, \quad (44)$$

and μ was set to 0.05. At last, ρ was set based on implementations to the helicopter, resulting 10^{-12}. Final target and recovered loops are also displayed in Figure 7.

IV. Simulation and Results

The system was first simulated using Matlab/Simulink. Two responses were tested: step and sinusoidal tracking. The former test procedure can be described as:

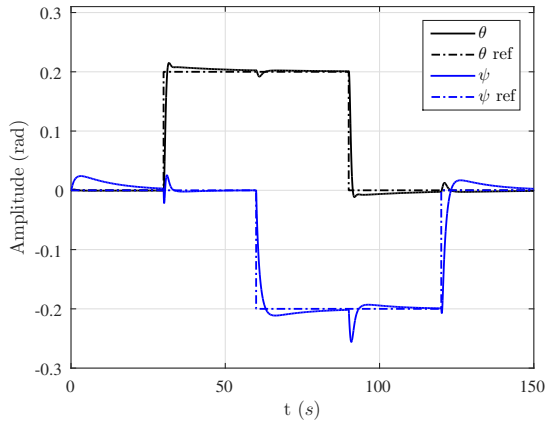

Fig. 8. System outputs for non-linear model simulation following step test procedure. θ and ψ are in rad, standing for pitch and yaw, respectively.

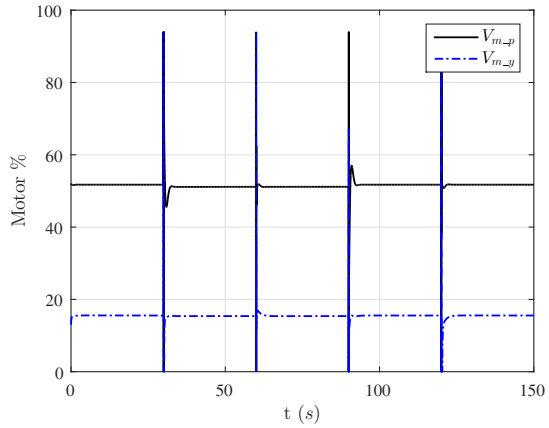

Fig. 9. Motors percentage for non-linear model simulation following step test procedure.

- wait 30s for system stabilization;
- give pitch a 0.2rad step input at 30s and -0.2rad step at 60s for yaw;
- bring both angles back to zero at 90s and 120s, respectively.

Simulation results for this procedure are shown in Figures 8 and 9. For sinusoidal input, it was chosen to use a sine with frequency of 0.04rad/sec, 0.35rad of amplitude for pitch and -0.2rad for yaw. Responses of this simulation are in Figures 10 and 11.

Using Freescale FRDM-K64F, an ARM based development platform, the controller was implemented and tested for both simulated inputs. Step responses are shown in Figures 12 and 13, while sinusoidal ones are in Figures 14 and 15.

The system showed a slightly different response from simulation, mainly in overshoots for step inputs and also a higher coupling. Besides this fact, the proposed controller was able to stabilize the system even far from linearization point. It is important to highlight the fact that the tests proved the barriers proposed in Figure 7 were satisfied. Lastly, as control effort for real tests are noisy, a 10-sample moving average filtering is also shown to emphasize its real trend.

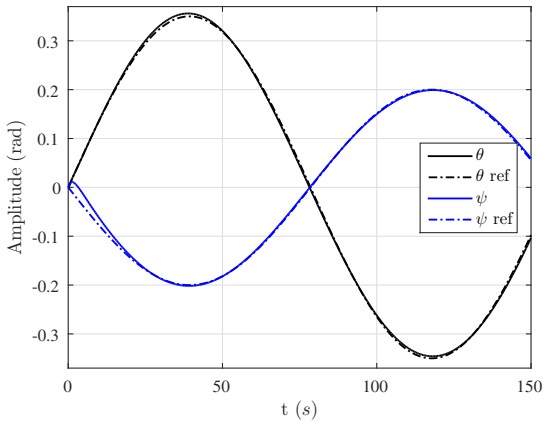

Fig. 10. System outputs for non-linear model simulation following sinusoidal input procedure. θ and ψ are in rad, standing for pitch and yaw, respectively.

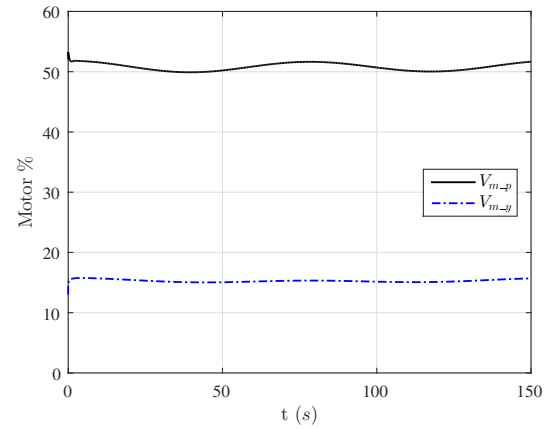

Fig. 11. Motors percentage for non-linear model simulation following sinusoidal input procedure.

V. Conclusion

It was shown the complete development of the discrete version of the LQG/LTR controller and how to augment it with integrators without missing the recovery. A 2DOF Helicopter was used to evaluate the controller, and its modeling was also shown.

The figures presented in previous sections show the system acting as it was projected to. It was able to reject disturbances at the output with frequencies below 0.15 rad/s and error not greater than 5%. Adding up, it was also able to follow sinusoidal reference with less than 3% of error.

Future works consist in better system identification for parameters as inertia and air resistance. Besides, different control techniques and new sensors might be implemented.

References

[1] Quanser, *Quanser 2-DOF Helicopter - Laboratory Manual*, 2nd ed., Quanser Inc., 2011.

[2] M. Guarnizo, R. Trujillo, and M. Guacaneme, "Modeling and control of a two dof helicopter using a robust control design based on dk iteration," in *IECON 2010 - 36th Annual Conference on IEEE Industrial Electronics Society*, Nov 2010, pp. 162–167.

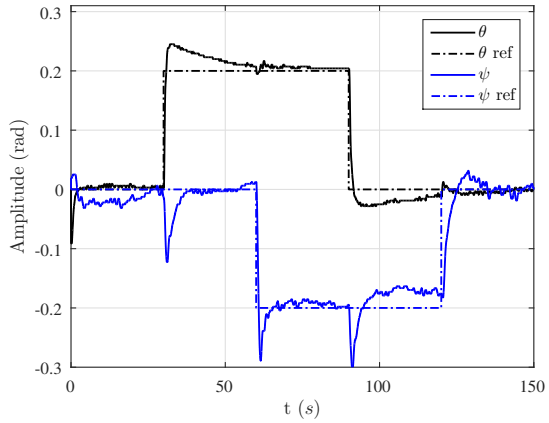

Fig. 12. Real system pitch and yaw following step test procedure.

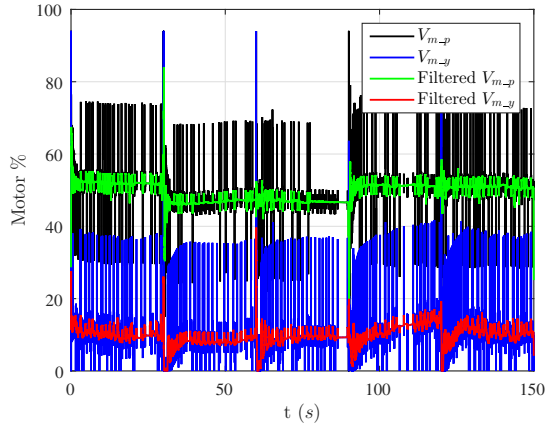

Fig. 13. Motors percentage for real system following step test procedure. Filtering was made using moving average of 10 samples.

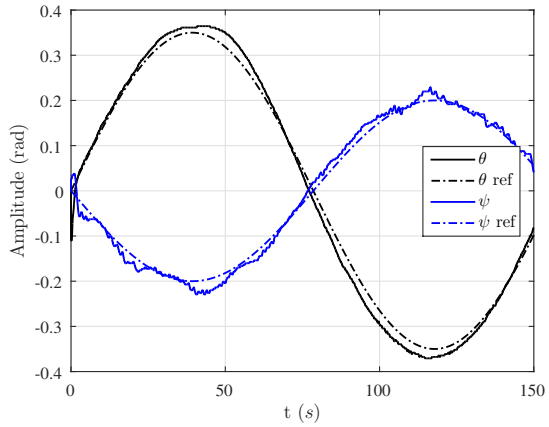

Fig. 14. Real system outputs for sinusoidal input procedure.

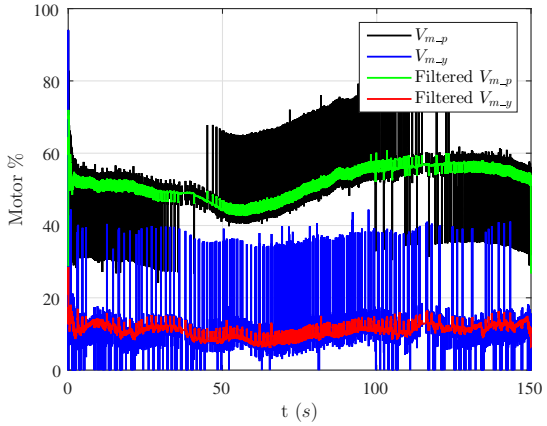

Fig. 15. Motors percentage for real system following sinusoidal input procedure. Filtering was made using moving average of 10 samples.

[3] K. Camacho, J. Burgos, and L. Combita, "Construction and modeling of a two-degree-of-freedom helicopter," in *Robotics Symposium and Latin American Robotics Symposium (SBR-LARS), 2012 Brazilian*, Oct 2012, pp. 150–155.

[4] E. Gonzalez, D. Rivera, and E. Gomez, "Model and observer-based controller design for a quanser helicopter with two dof," in *Electronics, Robotics and Automotive Mechanics Conference (CERMA), 2012 IEEE Ninth*, Nov 2012, pp. 267–271.

[5] C. Perez-D'Arpino, D. Vigouroux, W. Medina-Mele?ndez, L. Fermin, R. Torrealba, J. Grieco, and G. Fernandez-Lopez, "Development of a low cost inertial measurement unit for uav applications with kalman filter based attitude determination," in *Technologies for Practical Robot Applications (TePRA), 2011 IEEE Conference on*, April 2011, pp. 178–183.

[6] M. A. Khanesar, E. Kayacan, and O. Kaynak, "Optimal sliding mode type-2 tsk fuzzy control of a 2-dof helicopter," in *IEEE International Conference on Fuzzy Systems (FUZZ-IEEE)*, Aug 2015, pp. 1–6.

[7] J. C. Doyle, "Guaranteed margins for lqg regulators," *IEEE Transactions on Automatic Control*, vol. 23, no. 4, pp. 756–757, Aug 1978.

[8] J. C. Doyle and G. Stein, "Multivariable feedback design: Concepts for a classical/modern synthesis," *IEEE Transactions on Automatic Control*, vol. 26, no. 1, pp. 4–16, Feb 1981.

[9] G. Stein and M. Athans, "The lqg/ltr procedure for multivariable feedback control design," *IEEE Transactions on Automatic Control*, vol. 32, no. 2, pp. 105–114, Feb 1987.

[10] S. Weerasooriya and D. Phan, "Discrete-time LQG/LTR design and modeling of a disk drive actuator tracking servo system," *IEEE Transactions on Industrial Electronics*, vol. 42, no. 3, pp. 240–247, Jun 1995.

[11] J. Maciejowski, "Asymptotic recovery for discrete-time systems," *IEEE Transactions on Automatic Control*, vol. 30, no. 6, pp. 602–605, Jun 1985.

[12] F. H. D. Guaracy, D. L. F. da Silva, and L. H. C. Ferreira, "On the properties of augmented open-loop stable plants using lqg/ltr control," *IEEE Transactions on Automatic Control*, vol. 60, no. 8, pp. 2172–2176, Aug 2015.

[13] G. Franklin, J. Powell, and M. Workman, *Digital Control of Dynamic Systems*, 3rd ed. Ellis-Kagle Press, 2006.

[14] J. M. Maciejowski, *Multivariable feedback design*, ser. Electronic systems engineering series. Wokingham, England Reading, Mass. Addison-Wesley, 1989.